Parametric Numerical Study of Seismic Slope Stability and Verification of the Newmark Method

68

Almaz Torgoev and Hans-Balder Havenith

Abstract

2D dynamic modelling of seismic slope stability is applied to a landslide-prone area in Central Asia, the Mailuu-Suu Valley, situated in the south of Kyrgyzstan. The calculations are made with models constructed from five long profiles located in the target area, presenting different geological, tectonic and morphological settings. These input data were extracted from a 3D structural geological model built with the GOCAD software. Geophysical and geomechanical parameters were defined on the basis of results obtained by multiple surveys performed in the area over the past 15 years. These include geophysical investigation, seismological experiments and ambient noise measurements. Dynamic modelling of slope stability is performed with the UDEC version 4.01 software that is able to compute deformation on the basis of discrete elements. Inside these elements pure elastic materials (similar to rigid blocks) were used. Various parameter variations were tested to assess their influence on the final outputs. The total parametric study involved more than 50 different models (about 400 computation hours). Preliminary results allow us to evaluate the influence of topography and geology on the amplification of Areas Intensity, which is a very important parameter needed for the computation of Newmark displacements using different GIS approaches [Jibson et al. (US Geol Surv Open file report 98–113,1998); Miles and Ho (Soil Dyn Earth Eng 18:305–323,1999), among others]. The final results of our studies should allow us to define

A. Torgoev (✉)
Georisks and Environment, Department of Geology,
University of Liege, 4000 Liege, Belgium

A. Torgoev · H.-B. Havenith
GEOPRIBOR, Institute of Geomechanics and
Development of Subsoil, 720035 Bishkek,
Kyrgyz Republic

K. Ugai et al. (eds.), *Earthquake-Induced Landslides*,
DOI: 10.1007/978-3-642-32238-9_68,

the limitations of the simplified GIS-based Newmark displacement modelling; thus, the verified method would make landslide susceptibility and hazard mapping in seismically active regions more reliable.

Keywords
Tien shan · Landslides · Dynamic modelling · Amplification · Areas intensity · Newmark displacement

1 Introduction

The Mailuu-Suu River Valley is characterized by a combination of geological and tectonic settings favouring intense landslide activity in this area (Alioshin and Torgoev 2000; see landslides as dotted light areas in Fig. 68.1). Together with the hazardous environmental situation due to the presence of radioactive tailings close to some active mass movements, landslide activity itself poses significant risk to society. During the last years significant efforts from responsible agencies, such as the Ministry of Emergency Situation, were spent on environmental risk reduction measures. These efforts also take into account the possibility of a regional environmental catastrophe caused by landslide failure, uranium waste tailing destruction and penetration of radioactive material to Mailuu-Suu River flowing to the densely populated Fergana Valley. But, the effectiveness of risk reduction measures strongly depends on results of landslide hazard and risk studies, because some measures, like the removal of radioactive material and its transportation to another site, demand reliable estimation of landslide hazard in any new place of radioactive material disposal.

Nowadays GIS-based methods of landslide susceptibility mapping are widespread because of the relative low costs and the better effectiveness. But, in a lot of cases such kinds of approaches are suffering from over-simplification and need a deeper review of applied techniques. The goal of the current study is to verify the simplified Newmark displacement method developed on the basis of the original Newmark method (Newmark 1965) and adapted for GIS analyses (Jibson et al. 1998; Miles and Ho 1999, among others). Numerical simulations are applied to five long profiles passing through different landslides to compute seismically induced displacements. These results are compared with those obtained by GIS spatial analysis based on the simplified Newmark approach. Further perspectives include 3D dynamic modelling of a landslide site situated in another study area, the valley of Min-Kush River. This site was investigated by geophysical and seismological methods, which together with ongoing displacement monitoring allow us to compare displacements caused by real seismic events with those obtained by numerical simulations and by simplified GIS-based approaches. Fig. 68.1 presents the geological map of the target area in Mailuu-Suu river valley together with profiles indicated on this map.

The northern slopes of the Maily-Say Valley are mainly made up of Paleozoic and partly of Jurassic rocks (Formations CALI and JUCLA in Fig. 68.1) while the foothills in the south are formed by Tertiary sedimentary rocks. The central part of the valley hosting the town of Maily-Say shows a series of folds. The cores of the open anticlines are made of soft siltstone and sandstone (Cretaceous rocks: formations RED, LIGH and SALM) overlain by alternating by Paleogene to Neogene claystone and limestone (Formation LIM, PURP and MAIL in Fig. 68.1). On the basis of a new geological map, the slope instability distribution in the Maily-Say Valley was compared with the geologic setting. The comparison indicates that the highest landslide density is observed for the Purp Formation made of Paleogene claystone. The directly underlying LIM Formation made of Paleogene limestone is the second most susceptible formation to landslide processes. Field observations confirmed that landslides are generally located within soft

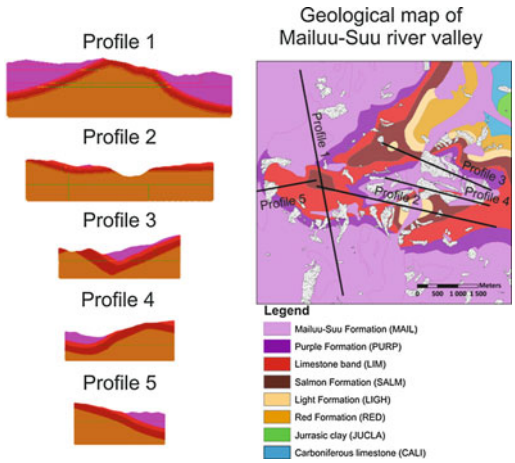

Fig. 68.1 Geological map of Mailuu-Suu river valley with landslides and profiles indicated

sediments composed of clay material or loess overlying the limestone layers. The fieldwork revealed that many slope instabilities have their head-scarps in the limestone layers. This means that they were initiated there, but affected mostly material of the adjacent units. Landslide occurrence also spatially correlates with structural and morphological factors, such as strike-and-dip of the limestone layers, the slope aspect, slope angle, and curvature.

The landscape in the Maily-Say Valley is continuously changing owing to the high landslide activity. The extent of this potentially dangerous evolution was quantified statistically. The total area affected by landslides increased from 1.0 % ($\sim$1.2 km^2) in 1962 to 3.3 % in 1984, 4.5 % in 1996, 4.3 % in 2002 and 5.6 % ($\sim$6.5 km^2) in 2007 compared to the entire investigated area along the Maily-Say Valley. Landslide size is quite variable; it ranges from 335 m^2 for the smallest detected landslide to 348,425 m^2 for the largest one in 2007. Further, the results indicate that the absolute number of large and very large landslides increases over time while the absolute number of small landslides decreases.

In this area, only a few co-seismically triggered landslides are known. However, several post-seismic landslides are likely to be related to partial co-seismic slope failure. Indeed, one of the largest landslides called 'Tektonik' first failed massively in 1992, seven weeks after a local Ms = 6.2 earthquake. Another, small landslide was monitored during several years and fracture opening of several tens of centimetres during a distant Ms = 5.9 earthquake could be proved at the end of the 90. In 2005, this slope finally failed to produce a 700 m-long earthflow made of loess.

2 Dynamic Modelling Settings

Modelling was performed with the UDEC software (version 4.01) combining computation with discrete elements (allowing for detachment or sliding of blocks along joints) and finite difference zones (filling the blocks and allowing for elastic or elasto-plastic deformation of the bulk material).

Topographic settings of constructed models were defined using DEM with cell size 20 × 20 m, obtained from SPOT satellite imagery in target area (Schlogel et al. 2010). Geological and tectonic settings were defined using a geological map of scale 1:10,000 together with 3D geological model of central part of area (Schlogel et al. 2010). In many cases, initial profiles were extended to a distance of 3–5 km to avoid boundary effects during dynamic modelling. The upper parts of all models with a depth down to 300–500 m were filled with FD-zones using an edge length of 7.5 m, while zones in the lower parts of models have an edge length of 15 m. All external boundaries, besides the surface, were designed to have viscous damping in x- and y-directions to avoid refraction effects during dynamic loading. The materials used in the models were those presented by the geological map and the 3D geological model. Some of the geological layers were integrated into one group according to the similarity of the geotechnical properties (Table 68.1). Dynamic properties of internal contacts (joint normal stiffness and joint shear stiffness) were assigned on the basis of the shear modulus of the upper layer in contact. At the beginning, all constructed profiles were cycled to obtain an unbalanced force value of less than 10^{-5} N. The stabilized profiles were subjected to

Table 68.1 Geotechnical settings of different material types used in dynamic modelling

Material code	Geological code	Cohesion, MPa	Friction angle, deg	Density, kg/m^3	Vp, m/sec	Vs, m/sec	Bulk modulus, MPa	Shear modulus, Mpa
Mat1	Purp, Mail (paleogene-neogene loose sediments)	0.04	26	2200	1000	500	1467	550
Mat2	Lim (limestone layer with average thickness of 100 m)	0.1	30	2400	4000	2200	22912	11616
Mat3	Salm (cretaceous loose sediments with average thickness of 155 m)	0.03	30	2200	1500	800	3073	1408
Mat4	Ligh, Red (cretaceous bedrock)	0.08	30	2200	2500	1300	9592	4056

dynamic loading using a Ricker wavelet as vertically (from the model base) propagated input signal. The maximum value of acceleration of the input signal was about 1.44 m/sec^2 (0.15 g) and the spectral range of the input signal was between 0.3 and 9.0 Hz. The duration of dynamic loading was 15 s—within this period of time the recording of different dynamic properties (acceleration, velocity and displacement of ground motion) was recorded by several receivers situated along the surface of model. Obtained recordings were analysed to compute the values of Areas intensity (Ia) recorded in those points. All models were analysed using two different cases—the case of unique material all over the model and the case of varying (real) geological materials. The first case was used to analyse pure topographic effects on the seismic amplification (with respect to a receiver on a flat hard rock site) of Areas intensity (At), while the second case presented the mixed effects of geology and topography on the seismic amplification of this parameter (Atg). Later, obtained values of seismic amplification were analysed to link this value with topographic parameters (curvature, slope angle, elevation) and geological settings. Five long profiles were analysed with a total length of 18.23 km and 101 receivers providing recordings of physical parameters

3 Analyses of Area Intensity Amplification Factor

3.1 Topographic Effect

There were some research attempts used to study effect of topography and geology on amplification of input seismic signal (Geli et.al. 1988; Jibson et.al. 1998; Miles and Ho 1999; Peng et.al 2009)—the results of these activities inspired some attempt of our research. Pure topographic amplification factors (At) for each receiver were obtained by dividing the Ia value in this point by the one obtained for the point situated close to the model basis (from which the ground motion was propagated). Some receiver points were not taken into consideration due to artificial shaking effects

generated along layer contacts and external boundaries. The remaining majority of points were used to relate At with topographic parameters, like curvature, slope angle and elevation.

Figure 68.2 presents correlations between these topographic features and pure topographic amplification factors obtained through numerical modelling. As it can be seen from Fig. 68.2a, concave topography favours to deamplification of Areas Intensity down to 60 % of initial values of Ia, while convex topography amplifies initial Ia values up to 80 %. Flat topography does not bring any effect on Ia amplification, which means At = 1. Figure 68.2b indicates that steeper slope angles favour deamplification of Ia, which generally was also found by former related research (Havenith and Bourdeau 2010; Danneels et. al. 2008; Geli et al. 1988). These three topographic parameters were used to obtain predicted values of pure topographic amplification of Areas Intensity (Atcalc). Formula (1) presents this relationship.

$$\begin{aligned}\text{Atcalc} = &\left(0.6037 * \text{C}^3 + 0.3225 * \text{C}^2 + 0.42\right. \\ &* \text{C} + 1.0468) * \left(0.5352 * \exp^{-0.0069 * \text{S}}\right) \\ &* \left(2 * 10^{-9} * \text{E}^3 - 5 * 10^{-6} * \text{E}^2 + 6 * 10^{-3}\right. \\ &* \text{E} - 1.5571)\end{aligned} \tag{68.1}$$

where C curvature, S slope angle (deg), E elevation (m)

The correlation coefficient between At and Atcalc was 0.87, which indicates a good prediction for this relationship. Figure 68.3 presents the comparison between At and Atcalc.

3.2 The Effect of Geology

Pure geological amplification factor (Ag) was obtained by subdividing of amplification values gained for combined effect of geology and topography (Atg) on ones for pure topographic case (At). In the analyses of Ag there were around 50 % of points filtered out owing to different artificial effects caused along contacts and boundaries in the model. Remaining points were used to calculate predicted amplification factors purely affected by the material type (Agcalc). Table 68.2 presents the results of Agcalc estimation. As it can be seen from this Table, the highest values of Ia amplification are presented by material 3 (mean value—2.86), which is explained by the structural and geomechanic characteristics of this layer. In general, this layer of soft, low-velocity material is "sandwiched" between two hard layers, which normally leads to wave focusing and consequently to high values of Areas Intensity. Material 1 also has comparatively high values of Ag (1.73), which can be explained by the fact that this layer is the softest one. However, along all profiles it is located above the hard limestone that may have some "screen" effect on wave propagation, reflecting waves back into material 3, Salm. Therefore, this layer made of the softest material 1 does not present the highest amplification. Pure geological deamplification in the material 2 is caused by the presence of high-velocity material between two low-velocity ones. Material 4 in our modeling was considered to be the bedrock and there is slight, but not significant amplification in this layer.

3.3 Combined Effect of Topography and Geology

Predicted values of combined amplification factor affected by both topography and geology (Atgcalc) were calculated as multiplication of topographic amplification factor (Atcalc) by geological one (Agcalc). Real values of combined amplification factor (Atg) have a correlation coefficient 0.75 with predicted values of this parameter (Atgcalc). This still indicates a good relationship between constructed relationship and observed values of this parameter. Figure 68.4 presents the plot of Atg versus Atgcalc.

4 Conclusions and Perspectives

The goal of this study is to integrate the results concerning the Arias Intensity and its amplification factors into the calculation of Newmark displacement. At present, the various modified

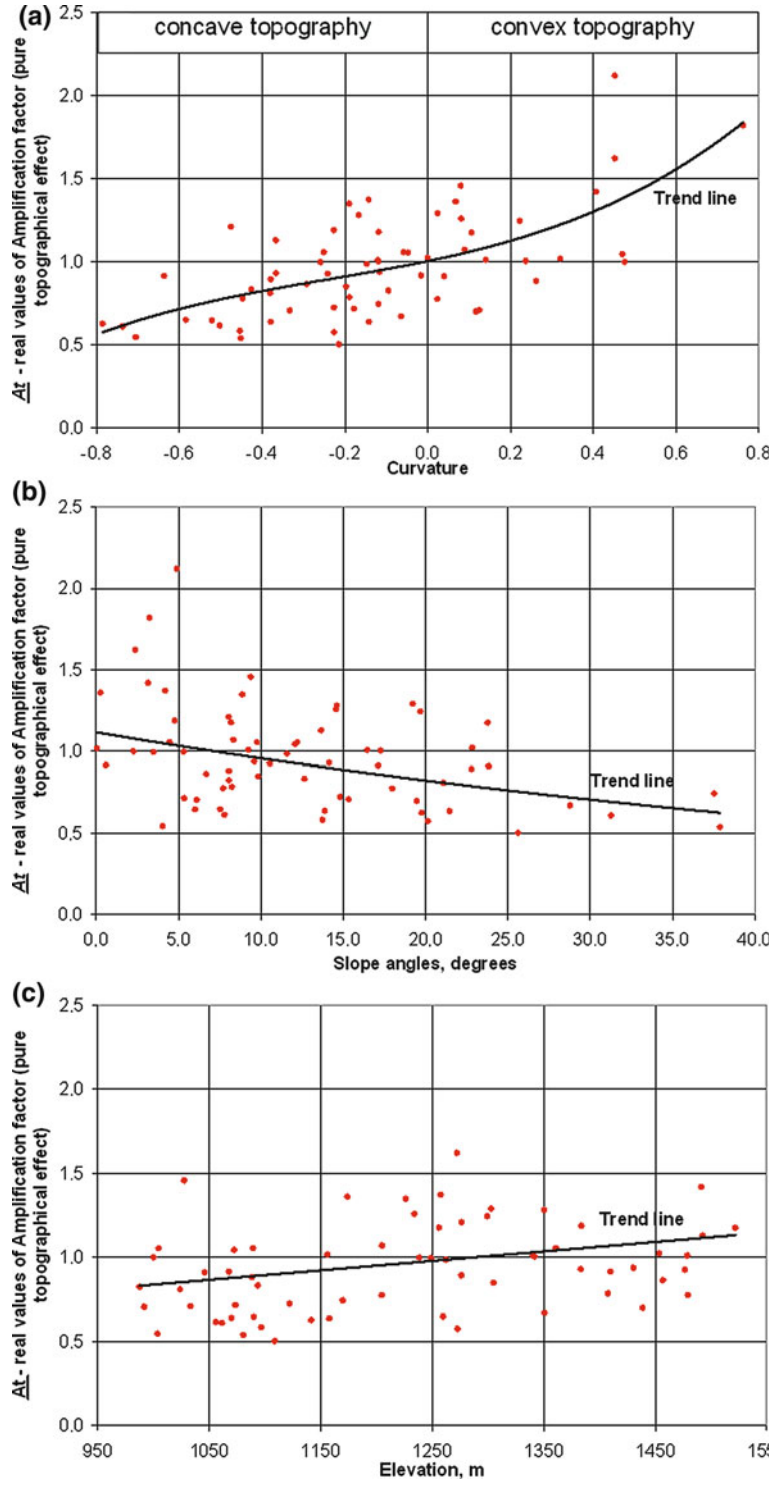

Fig. 68.2 The plots of real values of amplification factors (At) versus: *a* curvature; *b* slope angle; *c* elevation

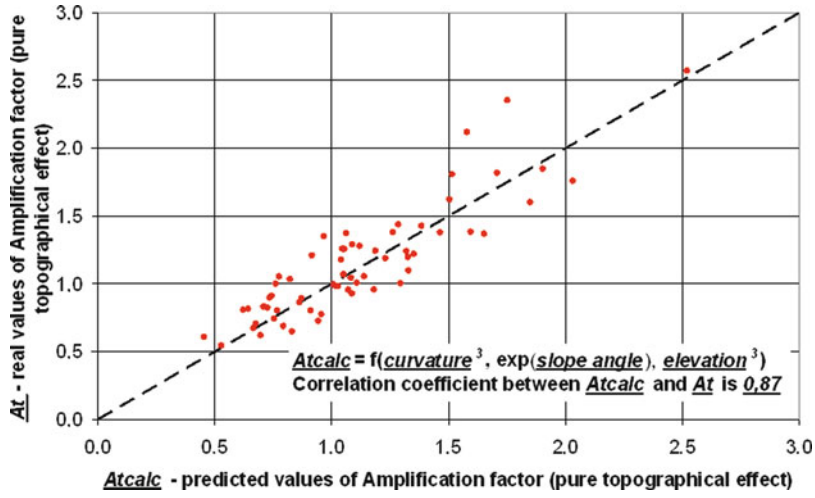

Fig. 68.3 The plot of real values of amplification factors (At) versus predicted values of amplification factor (Atcalc) for pure topographic effect

Table 68.2 Predicted values of amplification factors (Agcalc) purely affected by material type

Material code	Mean value of predicted amplification factor	Standard deviation for predicted amplification factor	Number of receivers analysed
Mat1	1.73	0.43	22
Mat2	0.81	0.25	9
Mat3	2.86	0.67	14
Mat4	1.19	0.15	5

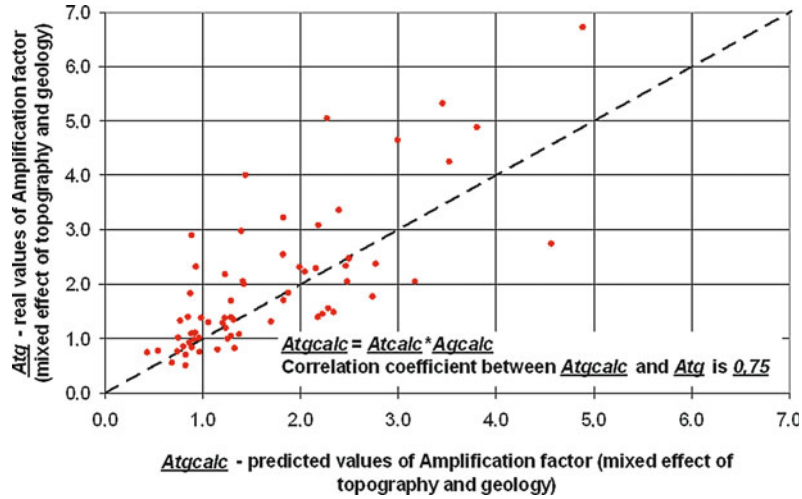

Fig. 68.4 The plot of real values of combined amplification factors (Atg) versus predicted values of amplification factor (Atgcalc) for combined effect of topography and geology

Newmark approaches consider only regionally varying Ia values (due to seismic wave attenuation from the epicenter). Such kind of prediction of amplification factor of Ia (here called 'Atgcalc') can easily be integrated into the widely used GIS-based analyses of seismic landslide susceptibility mapping. To be able to do so, the perspectives of our current activity involve more extended numerical studies in the target area both in the elastic and elasto-plastic domain. Elasto-

plastic dynamic modelling allows us to compare obtained values of displacements with those calculated with the Newmark displacement method (some preliminary tests have been started). Another perspective of the current activity also includes 3D dynamic numerical modelling of a target site situated in another area, where real seismic events caused certain amount of displacement in different parts of the landslide. This site was also studied from seismological and geophysical points of view, which finally give more reliable estimates of input parameters and provide good verification of obtained results. Final results of current study should make the Newmark displacement method more reliable in the mapping of landslide susceptibility in different parts of the world.

References

Alioshin Y, Torgoev I (2000) Radioactive ecology of Mailuu-Suu: Bishkek -Ilim

Danneels G, Bourdeau C, Torgoev I, Havenith HB (2008) Geophysical investigation and numerical modelling of unstable slopes: case-study of kainama (Kyrgyzstan). Geophys J Int 175:17–34

Geli L, Bard PY, Jullien B (1988) The effect of topography on earthquake ground motion: a review and new results. B Seismol Soc Am 78(1):42–62

Havenith HB, Jongmans D, Abdrakhmatov K, Trefois P, Delvaux D, Torgoev I (2000) Geophysical investigation of seismically induced surface effects : case study of a landslide in the Suusamyr valley, Kyrgyzstan. Surv Geophys 21:349–369

Havenith HB, Jongmans D, Faccioli E, Abdrakhmatov K, Bard PY (2002) Site effects analysis around the seismically induced ananevo rockslide, Kyrgyzstan. B Seismol Soc Am 92:3190–3209

Havenith HB, Bourdeau C (2010) Earthquake-induced hazards in mountain regions: a review of case-histories from Central Asia. Geologica Belgica 13:135–150

Jibson RW, Harp EL, Michael JA (1998) A method for producing digital probabilistic seismic landslide hazard maps: an example from Los Angeles, California, Area, US Geol Surv Open-file Report 98–113

Miles SB, Ho CL (1999) Rigorous landslide hazard zonation using newmark's method and stochastic ground motion simulation. Soil Dyn Earth Eng. 18:305–323

Nadim F, Kjekstad O, Peduzzi P, Herold C, Jaedicke C (2006) Global landslide and avalanche hotspots. Landslides 3:159–173

Newmark N (1965) Effects of earthquakes on dams and embankments. Geotechnique 15(2):139–160

Peng W-F, Wang C-L, Chen S-T, Lee S-T (2009) A seismic landslide hazard analyses with topographic effect study in the 99 peak region, Central Taiwan. Environ Geol 57:537–549

Schlogel R, Torgoev I, De Marneffe C, Havenith H-B (2010) Assessment of landslide activity in the Maily-Say Valley, Kyrgyz Tien Shan. Earth Surf Proc Land 36(12):1658–1669